

Figure 6. Planar image reconstructions of the ^{18}F -sources in the tumor phantom of figure 3(b). Shown are the results for three phantom positions relative to the isocenter and at the acquisition times of 1, 3 and 5 min, respectively.

Table 1. Statistical comparison of registration errors from PDRI and radiographic registrations using ANOVA. PDRI registration was performed using reconstructed planar images from PET data (at the acquisition time of 15 min) and BOLPs data (at the acquisition times of 1, 3 and 5 min). Radiographic registration was performed using DRR and portal (x-ray) images.

Registration method	Diameter				
	8 mm	12 mm	16 mm	25 mm	32 mm
PDRI (1 min)	1.07 ± 0.42	0.49 ± 0.34	1.02 ± 0.44	1.28 ± 0.35	1.12 ± 0.39
PDRI (3 min)	0.87 ± 0.29	0.59 ± 0.24	1.01 ± 0.38	1.25 ± 0.29	0.86 ± 0.37
PDRI (5 min)	0.56 ± 0.26	0.60 ± 0.24	1.00 ± 0.34	1.30 ± 0.26	0.88 ± 0.32
Radiographic (x-ray)	0.98 ± 0.28	0.63 ± 0.30	0.87 ± 0.31	0.95 ± 0.20	1.17 ± 0.26
<i>p</i> -value	$<0.0001^*$	0.3545	0.522	0.0003^*	0.0044^*

*Significant ($p < 0.05$).

registration errors and a relatively smaller registration error for the radiographic registration. However, the difference between the PDRI and radiographic registrations was found to be statistically significant only for 24 mm at $p = 0.0003$. A significant difference between the PDRI and radiographic registration errors was obtained for the 32 mm diameter.

The statistical comparisons of the mean registration error and SD for each source diameter obtained from the PDRI registration at 1, 3, and 5 min and the radiographic registration are shown in figures 8 and 9.

For the diameter of 8 mm, the differences in the registration error for the three acquisition times used in the PDRI registration were found to be statistically significant. However, when compared to the registration error of the radiographic registration, only the 5 min PDRI data yielded a significant difference. The mean registration errors for the image registration

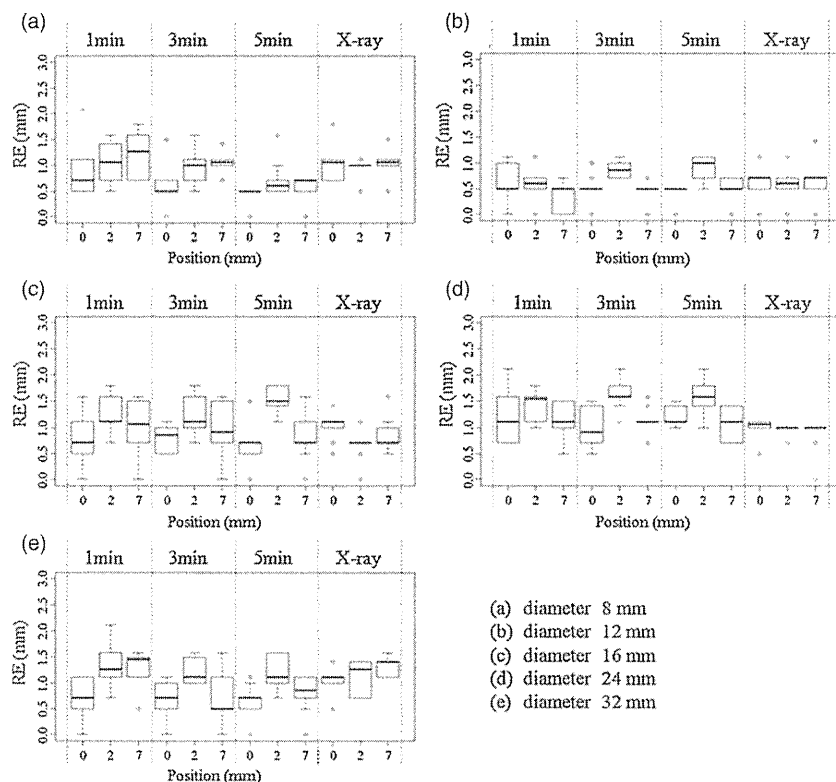


Figure 7. Registration errors for the tumor phantom of figure 3(b). Shown are the results for three phantom positions relative to the isocenter (0), isocenter + 2 mm (2) and isocenter + 7 mm (7) at the acquisition times of 1, 3 and 5 min, respectively.

conditions shown in figures 8(b) and (c) for diameters of 12 and 16 mm were not statistically different. However, a larger variation in the computed registration error was observed for 16 mm.

For the diameter of 24 mm, the mean registration error obtained for the radiographic registration was found to be significantly smaller compared to those obtained using the PDRI registration method. Furthermore, the acquisition time did not appear to result in significant differences in the mean registration error for the PDRI registration. Like those of the results for the 8 mm diameter, the mean registration error for the 32 mm diameter decreased with the acquisition time in the PDRI registration.

A comparison of the registration error SDs is shown in figure 9 for the various diameters and data acquisition methods. The SDs for most of the results were not statistically different. The image registration SDs of the PDRI at 3 min acquisition time were statistically the same as those of the radiographic registration.

4. Discussion

An overall evaluation of the accuracy of PDRI registration independent of the source size is necessary. We therefore performed a comparative study of the registration error obtained with PDRI and radiographic registrations for a number of hypothetical source sizes. The cumulative

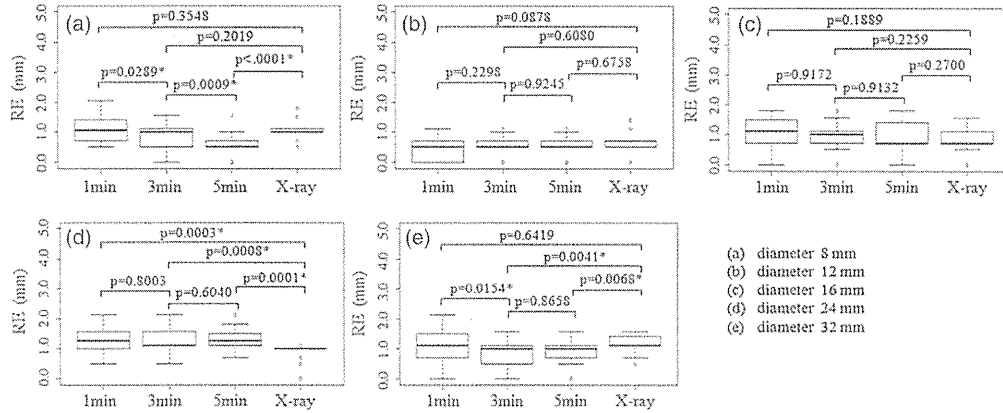


Figure 8. Statistical comparison of the mean registration error for the five cylindrical sources with diameters of 8, 12, 16, 24 and 32 mm using Student's *t*-test at $p < 0.05$ significance level.

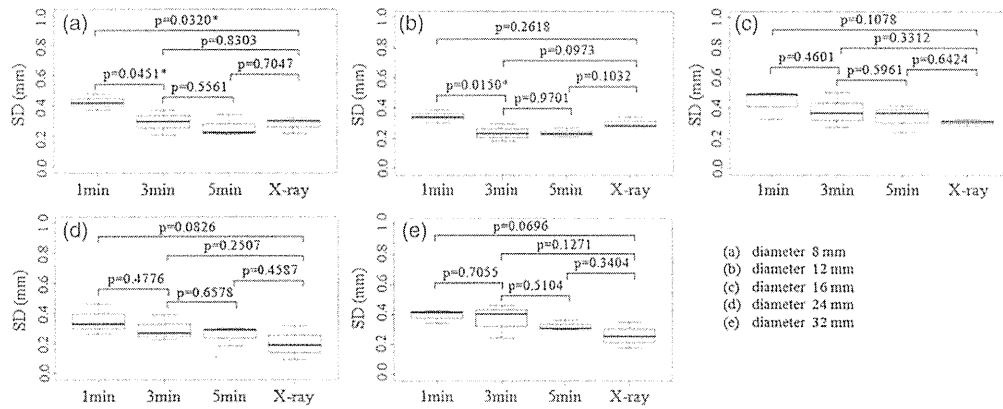


Figure 9. Statistical comparison of the standard deviation of the mean registration error for the five cylindrical sources with diameters of 8, 12, 16, 24 and 32 mm using Student's *t*-test at $p < 0.05$ significance level.

mean registration error and SD for five different source sizes using four registration conditions (i.e. PDRI at 1, 3 and 5 min acquisition times and radiographic registration) are shown in figure 10. A general trend of decreasing mean registration error and SD for longer acquisition time is seen for the PDRI registration. The 3 min data acquisition in the BOLPs yielded comparable results to radiographic registration, while the 5 min acquisition appears to result in lower registration error.

Our tumor phantom experiments show that the mean of the registration errors for the PDRI is approximately 0.93 mm and the SD is approximately 0.33 mm. This is not statistically different from the radiographic registration which had a mean registration error of 0.92 ± 0.27 mm.

Although there are no reports on the accuracy of image registration using molecular imaging, there have been a number of publications regarding the accuracy of DRR and EPID image registration. Dong and Boyer (1995) showed that in their phantom image registration study, the correlation procedure had a SD of 0.5 mm in aligning translational shifts. Gillhuijs

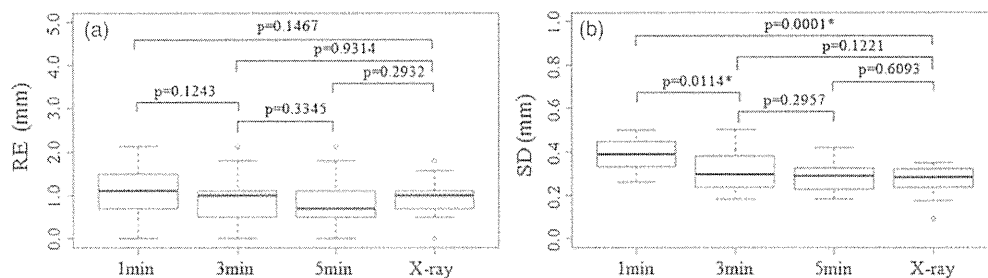


Figure 10. Statistical comparison of (a) the mean registration error and (b) the standard deviation for an overall evaluation using Student's *t*-test at $p < 0.05$ significance level.

et al (1996) registered 2D portal images with CT data, and their automatic 3D analysis of patient setup accuracy was found to be accurate to within 1 mm in the translational directions. In the clinical evaluation of patient setup errors using portal imaging by Hurkmans *et al* (2001), it was reported that setup errors were less than 2.0 mm (1SD) for head and neck, 2.5 mm (1 SD) for prostate, 3.0 mm (1 SD) for general pelvic and 3.5 mm (1 SD) for lung cancer. The study also noted that the setup verification accuracy varies widely, depending on the treatment site, method of immobilization and institution.

The registration error for the PDRI was lower than that of previously reported radiographic registrations. This could be due to the fact that the image registration was performed with ^{18}F -source itself, not with the skeletal structure, or that there was a phantom dependence. Nevertheless, the registration error for PDRI registration was not significantly different from that of radiographic registration in our experiments. As shown in figure 10(b), the registration error is dependent on the data acquisition time. In order to apply PDRI registration clinically, the acquisition time should be taken into account. A longer acquisition time will result in lower registration error, but it will cause patient discomfort. An optimum acquisition time needs to be considered while maintaining the registration accuracy. However, this is complicated because it depends on the tumor and normal tissue uptake and radiation attenuation in the patient's body. Patient immobilization may also be necessary in order to minimize the effects of inter- and intra-fraction motion caused by patient movement. The effect of respiratory induced motion should be considered in future works.

If FDG is used as the tracer in PDRI registration, it will also be taken up in normal organs such as the brain, liver, kidneys, bladder, etc. This will be a problem in this image registration modality. However, because of the high spatial resolution of our parallel-plane PET system along the in-plane direction, it should be possible to distinguish the tumor FDG uptake from that of the adjacent normal organs which also accumulate FDG. As shown in Figure 4, at the same gantry angle, the corresponding cross-plane image has a much lower resolution and therefore would not be usable for image registration.

Conventional radiographic registration is performed by taking a portal planar image in the LR direction with the gantry at 0° and afterward rotating the gantry to 90° in order to take another portal planar image at the AP direction. These left-right (LR) and anterior-posterior (AP) images are separately registered with corresponding DRR images to complete the radiographic registration process. In our m-IGRT system, the same setup verification procedure using LR and AP images taken separately at different gantry angles will have to be performed. In this case, the PDRI for the LR direction will be the reconstructed in-plane image from the parallel-plane PET data obtained at a gantry angle of 0° . On the other hand, the PDRI for the AP direction will be the reconstructed in-plane image from parallel-plane

PET data obtained at a gantry angle of 90°. The measurement time for each gantry angle is expected to be only a few minutes; therefore, the effects on the acquired parallel-plane PET data of metabolic changes in the body or source activity are negligible.

Additionally, this high spatial resolution will likewise be useful in hypoxic region imaging using FMISO because the hypoxic region distribution in the tumor is complex (Nehmeh *et al* 2008).

5. Conclusion

We performed a basic study to determine the accuracy of image registration using a PET-based molecular image guided method. Planar images were reconstructed from parallel-plane PET data to obtain the PET-based digitally reconstructed planar image (PDRI) used in the registration. In-plane PDRI had higher resolution and therefore usable for image registration. Phantom experiments using in-plane PDRI showed that there is no significant difference between radiographic and PDRI registrations. Our results suggest that m-IGRT image registration using PET-based reconstructed planar images along the in-plane direction is feasible for clinical use. Furthermore, the system will provide additional information for image registration when bony structures cannot be recognized with radiographic registration methods.

Acknowledgments

This research was a part of the 'Innovation COE Program for Future Drug Discovery and Medical Care' project and partially supported by the Grant-in-Aid for Special Coordination Funds for Promoting Science and Technology of the Japanese Ministry of Education, Culture, Sports, Science and Technology. The authors are also grateful to the assistance given by the Proton Radiotherapy Department of the National Cancer Center, Kashiwa staff during the experiments with the BOLPs. This research was partially supported by Health and Labour Science Research Grants from the Japanese Government.

References

- Dong L and Boyer A L 1995 An image correlation procedure for digitally reconstructed radiographs and electronic portal images *Int. J. Radiat. Oncol. Biol. Phys.* **33** 1053–60
- Ford E C, Chang J, Mueller K, Sidhu K, Todor D, Mageras G, Yorke E, Ling C C and Amols H 2002 Cone-beam CT with megavoltage beams and an amorphous silicon electronic portal imaging device: potential for verification of radiotherapy of lung cancer *Med. Phys.* **29** 2913–24
- Gilhuijs K G A, van de Ven P J H and van Herk M 1996 Automatic three-dimensional inspection of patient setup in radiation therapy using portal images, simulator images, and computed tomography data *Med. Phys.* **23** 389–99
- Groh B A, Siewerdsen J H, Drake D G, Wong J W and Jaffray D A 2002 A performance comparison of flat-panel imager-based MV and kV cone-beam CT *Med. Phys.* **29** 967–75
- Hoffman E J *et al* 1989 PET system calibrations and corrections for quantitative and spatially accurate images *IEEE Trans. Nucl. Sci.* **36** 1108–12
- Huesman R H *et al* 2000 List-mode maximum-likelihood reconstruction applied to positron emission mammography (PEM) with irregular sampling *IEEE Trans. Med. Imaging* **19** 532–7
- Hurkmans C W *et al* 2001 Set-up verification using portal imaging: review of current clinical practice *Radiother. Oncol.* **58** 105–20
- Jaffray D A, Siewerdsen J H, Wong J W and Martinez A A 2002 Flat-panel cone-beam computed tomography for image-guided radiation therapy *Int. J. Radiat. Oncol. Biol. Phys.* **53** 1337–49
- Lee N Y and Le Q T 2008 New developments in radiation therapy for head and neck cancer: intensity-modulated radiation therapy and hypoxia targeting *Semin. Oncol.* **35** 236–50

- Lerche C W *et al* 2005 Depth of γ -ray interaction within continuous crystals from the width of its scintillation light-distribution *IEEE Trans. Nucl. Sci.* 52 560–72
- MacDonald L *et al* 2009 Clinical imaging characteristics of the positron emission mammography camera: PEM Flex Solo II *J. Nucl. Med.* 50 1666–75
- Munbodh R, Jaffray D A, Moseley D J, Chen Z, Knisely J P S, Cathier P and Duncan J S 2006 Automated 2D–3D registration of a radiograph and a cone beam CT using line-segment enhancement *Med. Phys.* 33 1398–411
- Nehmeh S A *et al* 2008 Reproducibility of intratumor distribution of ^{18}F -fluoromisonidazole in head and neck cancer *Int. J. Radiat. Oncol. Biol. Phys.* 70 235–42
- Nishio T *et al* 2005 Distributions of β^+ decayed nuclei generated in the CH_2 and H_2O targets by the target nuclear fragment reaction using therapeutic MONO and SOBP proton beam *Med. Phys.* 32 1070–82
- Nishio T *et al* 2006 Dose-volume delivery guided proton therapy using beam online PET system *Med. Phys.* 33 4190–7
- Nishio T *et al* 2010 The development and clinical use of a beam on-line PET system mounted on a rotating gantry port in proton therapy *Int. J. Radiat. Oncol. Biol. Phys.* 76 277–86
- Pouliot J *et al* 2005 Low-dose megavoltage cone-beam CT for radiation therapy *Int. J. Radiat. Oncol. Biol. Phys.* 61 552–60
- Raylman R R *et al* 2008 The positron emission mammography/tomography breast imaging and biopsy system (PEM/PET): design, construction and phantom-based measurements *Phys. Med. Biol.* 53 637–53
- Shepp L A and Vardi Y 1982 Maximum likelihood reconstruction for emission tomography *IEEE Trans. Med. Imaging.* 1 113–22
- Siddon R L 1985 Fast calculation of the exact radiological path for a three dimensional CT array *Med. Phys.* 12 252–5
- Smith M F *et al* 2003 Analysis of factors affecting positron emission mammography (PEM) image formation *IEEE Trans. Nucl. Sci.* 50 53–9
- Smith M F *et al* 2004 Positron emission mammography with tomographic acquisition using dual planar detectors: initial evaluations *Phys. Med. Biol.* 49 2437–52
- Som P *et al* 1980 A fluorinated glucose analog, 2-fluoro-2-deoxy-D-glucose (F-18): nontoxic tracer for rapid tumor detection *J. Nucl. Med.* 21 670–5
- Wienhard K *et al* 2002 The ECAT HRRT: performance and first clinical application of the new high resolution research tomograph *IEEE Trans. Nucl. Sci.* 49 104–10
- Yamaya T, Hagiwara N, Obi T, Yamaguchi M, Kita K, Ohyama N, Kitamura K, Hasegawa T, Haneishi H and Murayama H 2003 DOI-PET image reconstruction with accurate system modeling that reduces redundancy of the imaging system *IEEE Trans. Nucl. Sci.* 50 1404–9
- Zhang J *et al* 2007 Study of the performance of a novel 1 mm resolution dual-panel PET camera design dedicated to breast cancer imaging using Monte Carlo simulation *Med. Phys.* 34 689–702

Long-term Outcomes of Fractionated Stereotactic Radiotherapy for Intracranial Skull Base Benign Meningiomas in Single Institution

Shunsuke Onodera^{1,*}, Hidefumi Aoyama¹, Norio Katoh¹, Hiroshi Taguchi¹, Kouichi Yasuda¹, Daisuke Yoshida¹, Ken Surtherland², Ryusuke Suzuki², Masayori Ishikawa², Bengua Gerard², Shunsuke Terasaka³ and Hiroki Shirato²

¹Department of Radiation Medicine, Hokkaido University Graduate School of Medicine, ²Department of Medical Physics, Hokkaido University Graduate School of Medicine and ³Department of Neurosurgery, Hokkaido University Graduate School of Medicine, Sapporo, Japan

*For reprints and all correspondence: Shunsuke Onodera, Department of Radiation Medicine, Hokkaido University Graduate School of Medicine, North 15, West 7, Kita-ku, Sapporo 060-8638, Japan. E-mail: m950086@jasmine.ocn.ne.jp

Received May 6, 2010; accepted November 21, 2010

Objective: To investigate the outcome of linac-based fractionated stereotactic radiotherapy over the last 10 years for intracranial skull base benign meningiomas in patients who were inoperable, who had residual tumors with some components of high mitotic index after surgery and who experienced relapse of the tumor.

Methods: Twenty-seven patients with intracranial skull base benign meningiomas treated with fractionated stereotactic radiotherapy were retrospectively reviewed. Twenty-seven cases were diagnosed as benign meningiomas on pathological (17 cases) or radiological (10 cases) examination. The median follow-up time was 90 months after initial treatment and 63 months after fractionated stereotactic radiotherapy. The median biological equivalent dose calculated using an α/β ratio of 2.0 Gy was 82.0 Gy (range, 60–106 Gy).

Results: The 5-year overall survival was 95.7 (95% confidence interval: 87.3–100)% after initial treatment and 96.2 (88.8–100)% after fractionated stereotactic radiotherapy. The 5-year overall survival and local control rate of patients who received fractionated stereotactic radiotherapy alone were both 100%. The 5-year progression-free survival and local control rate after fractionated stereotactic radiotherapy were all 100% with a tumor volume of <9.1 cc and 68.2 (37.2–99.2) and 75.8 (45.2–100)% for the tumors 9.1 cc, respectively. The difference was significant in progression-free survival ($P=0.022$) and local control rate ($P=0.044$). The local control rate was significantly worse in patients who received fractionated stereotactic radiotherapy for relapsed tumors ($P=0.01$). No late radiation damage was observed in the follow-up period.

Conclusions: The long-term outcome suggests that fractionated stereotactic radiotherapy is a safe and effective treatment for intracranial skull base benign meningioma, especially for those who have tumors <9.1 cc or would receive fractionated stereotactic radiotherapy with or without surgery as the initial treatment.

Key words: radiation therapy – meningioma – stereotactic – skull base – fractionation

INTRODUCTION

Radiotherapy is increasingly being used for the treatment of meningiomas after incomplete resection, after recurrence and when tumor histology is atypical or malignant (1,2). When

meningiomas are located in the intracranial skull base region, tumor excision is frequently incomplete and even biopsy can be hazardous (1). Therefore, it is a matter of

debate whether the use of radiotherapy should be used when the residual tumor is still small as the primary treatment or should be reserved as a potential salvage treatment for the residual tumor enlarged (3).

Stereotactic radiosurgery (SRS) has been proven useful for reducing unnecessary irradiation to the normal tissue surrounding meningiomas and provides an excellent local control rate (LCR) for small to mid-size skull base meningiomas (3,4). Three-dimensional conformal radiotherapy (3D-CRT) and fractionated stereotactic radiotherapy (FSRT) are expected to be useful for further reducing the possibility of late adverse reactions, even for relatively large tumors (5,6). Although there were several precise reports from a few institutions about the long-term outcome after FSRT (5–8), we are still short of knowledge about the treatment results of FSRT with the median follow-up longer than 60 months for intracranial meningioma.

We began using FSRT 15 years ago for patients with intracranial skull base meningiomas, principally for patients who were inoperable, who had residual tumors with some components of high mitotic index or high MIB-1 index, who experienced relapse of the tumor. In this study, we retrospectively reviewed our long-term results for FSRT of intracranial skull base benign meningiomas in order to investigate the usefulness and prognostic factors of this treatment.

PATIENTS AND METHODS

PATIENTS

The outcome of 27 patients with intracranial skull base benign meningiomas treated with FSRT at Hokkaido University Hospital between May 1994 and February 2009 was retrospectively reviewed. Our treatment policy was to apply FSRT principally for those patients with intracranial skull base meningiomas who were inoperable, who had residual tumors or who experienced relapse of the tumor.

The patients' characteristics are summarized in Table 1, which were classified by the treatment category. In our cases, diagnosis was based on pathological examinations in 17 patients and radiological characteristics in 10 patients. The tumor was located at lateral structures in 17 (anterior fossa in 2, middle-lateral sphenoid wing in 8 and cerebello-pontine angle and posterior fossa in 7 patients) and at central structures in 10 patients (cavernous sinus and tuberculum sellae in all 10 patients). The median tumor volume was 9.1 (range: 1.1–86.1) cc in all benign meningiomas. The median tumor volume in the initial treatment group was smaller than that in the salvage treatment group (6.3 vs. 12.3 cc), but there was no significant difference statistically ($P = 0.139$; Mann–Whitney test).

In this study, 11 patients were treated with FSRT alone as the initial treatment: 1 after biopsy (Simpson's grade V) and 10 after radiological diagnosis. Radiotherapy was used as a part of the initial treatment after incomplete excision in 4 patients and as a salvage treatment for tumor recurrence

Table 1. Patients' characteristics

Factors	Initial treatment group	Salvage treatment group	Total
Total	15	12	27
Diagnosis			
Pathological diagnosis	5	12	17
Radiological diagnosis	10	0	10
Sex			
Male	1	6	7
Female	14	6	20
Age			
Mean (range)	60.3 (18–78)	45.5 (14–72)	53.7 (14–78)
Tumor site			
Lateral	11	6	17
Central	4	6	10
Gross tumor volume			
Median (range) (cc)	6.3 (1.1–58.9)	12.3 (2.5–86.1)	9.1 (1.1–86.1)
Simpson's grade			
I	0	0	0
II	0	1	1
III	0	0	0
IV	4	11	15
V	1	0	1
Radiotherapy alone	10	0	10

after surgery in 12 patients. The number of surgical procedures before FSRT was 1, 2 and 3 in 10, 5 and 1 patients, respectively. Patients who received open biopsy or surgery were classified according to Simpson's grade (9). Simpson's grade II (complete removal and coagulation of dual attachment) and IV (subtotal resection) surgery before radiotherapy was performed in 1 and 15 patients, respectively. Only one patient received biopsy (Simpson's grade V).

RADIATION THERAPY METHOD

The gross tumor volume (GTV) was taken as the gross tumor shown on computed tomography (CT) with or without magnetic resonance imaging (MRI). The clinical target volume (CTV) was equal to the GTV, post-operative tumor bed or both in this study. The planning target volume (PTV) was 2–3 mm geometric expansion of the CTV. In delineating GTV, MRI co-registered with CT was used in 18 recent patients, and only the CT information was used for the remaining 9 patients.

Treatment planning systems were Focus or Xio (CMS Japan, Japan). A dose calculation algorithm used for the skull base meningiomas was the Clarkson method or the

convolution method. Stereotactic radiotherapy was carried out by using a 6 or 10 MV linear accelerator (LINAC) (2100C: Varian, Palo Alto, CA, USA; EXL15DP: Mitsubishi, Japan) with an in-house developed LINAC-based SRT system. Three-dimensional non-coplanar, single isocenter and the technique using multileaf collimator (MLC) were used. Three to eight static non-coplanar ports with the conformal fields were used in general. The width of these leafs was 5–10 mm at the isocenter. The dose was prescribed at the isocenter and defined as 100% in the dose distribution profile. MLCs were opened to cover PTV by a 90–95% isodose shell. The maximum dose point was always situated near the isocenter with the dose $<110\%$ (Fig. 1).

Patients were fixed by using a thermo-plastic mask and a custom-made head rest system. The dose to the optic chiasm was limited to ≤ 46 Gy. The total dose was 48–54 Gy in 26 cases and 32 Gy in 1 case using 2.0 Gy as the daily dose. When these radiation schedules were converted into the biological equivalent dose (BED) using an α/β ratio of 2.0 Gy, the median BED dose was 82.0 Gy (range: 52–90 Gy).

FOLLOW-UP AND STATISTICAL ANALYSES

The median follow-up time was 90 months (range: 21–209 months) after initial treatment, surgery or FSRT. The median follow-up time was 63 months (range: 19–154 months) after FSRT. More than 70% of patients were followed longer than 36 months after FSRT. Patients were periodically monitored by physical as well as radiographic examination in Hokkaido University Hospital and related hospitals. Local tumor progression (PD) was scored when the maximum diameter of the tumor increased 2 mm or more and partial reaction was scored when the diameter decreased 2 mm or more. The LCR was defined as no change or decrease of the tumor volume in the anatomical region consistent with the PTV of the treatment planning image. When more than 80% of the relapsed tumor volume was outside of the PTV, the recurrence was defined as out of field (10). In-field ($>95\%$ of the relapsed tumor volume in the PTV), marginal (20–95% of the relapsed tumor volume in the PTV), and out-of-field (less than 20% of the relapsed tumor volume in the PTV) recurrence were defined in this study.

Statistical analyses were conducted by using commercially available software (SPSS v18; IBM Inc., Chicago, IL). The overall survival (OS) and LCR were calculated from the date

of the initiation of radiotherapy using the Kaplan–Meier method, and statistical evaluations were carried out by the log-rank test.

RESULTS

The OS, progression-free survival (PFS) and LCR at 5 years after initial treatment were 95.7 [95% confidence interval (CI): 87.3–100], 91.6 (80.4–100) and 95.5 (86.9–100)%.

The OS, PFS and LCR at 5 years after FSRT were 96.2 (88.8–100), 84.6 (67.7–100) and 88.6 (72.9–100)%.

Partial response was achieved in two benign patients, and the other patients with local control experienced no change of tumor volume. Three (11%) patients experienced in-field recurrence. These tumors had received Simpson's grade IV surgical resection. One patient had progression disease out of irradiation field. The recurrent cases were observed at the posterior fossa (at 55 and 81 months) in two patients, and at the cavernous sinus and tuberculum (at 19 and at 27 months) in two patients. These four recurrent cases are summarized in Table 2. No marginal recurrence was observed.

Univariate analyses were performed on OS, PFS and LCR after FSRT for patients with benign meningioma (Table 3). The female patients had significantly better PFS ($P = 0.009$) and LCR ($P = 0.04$) than the male patients. The 5-year OS, PFS and LCR after FSRT were all 100% for the benign meningiomas with a tumor volume of <9.1 cc and these parameters were 91.7 (76.0–100), 68.2 (37.2–99.2) and 75.8 (45.2–100)% for the tumors >9.1 cc, respectively. The difference was significant in PFS ($P = 0.022$) and LCR ($P = 0.044$) (Fig. 2).

In this study, the 11 patients who received FSRT alone had 100% OS, 88.9% PFS and 100% LCR at 5 years, respectively. The OS, PFS and LCR of patients who received FSRT with or without surgery as the initial treatment ($n = 15$) were 100, 91.7 and 100%, whereas those of patients who received FSRT for relapse ($n = 12$) were 90.9, 68.2 and 68.2%, respectively. The LCR was significantly worse in patients who received FSRT for a relapsed tumor ($P = 0.01$). A higher biological radiation dose, BED, was paradoxically associated with a lower PFS and LCR. The median tumor volume was larger (11.0 vs. 6.7 cc) and the ratio of patients with relapsed tumor was higher (7/11 vs. 5/16) in the higher



Figure 1. Dose distribution of FSRT for an intracranial benign meningioma. FSRT, fractionated stereotactic radiotherapy.

Table 2. The characteristics of patients with skull base benign meningioma who experienced tumor recurrence after FSRT either in-field or out-of-field

No.	Age	Sex	Primary site	Gross tumor volume (cc)	Simpson's grade	FSRT for relapsed tumor	Dose/fraction (Gy/fraction)	Local control	Recurrent site	Relapse (months)	Survival times	Final status
1	78	M	Cavernous sinus	58.9	Grade V	No	54 Gy/27fr	NC	Out-of-field	27	27	Alive
2	35	M	Cerebellopontine angle	9.75	Grade IV	Yes	54 Gy/27fr	PD	In-field	81	81	Alive
3	51	M	Cerebellopontine angle	13.9	Grade IV	Yes	44 Gy/22fr + 10 Gy/4fr	PD	In-field	55	55	Alive
4	58	F	Tuberculum sellae	24.9	Grade IV	Yes	54 Gy/27fr	PD	In-field	19	20	Death

FSRT, fractionated stereotactic radiotherapy; NC, no change; PD, progression of disease.

Table 3. The univariate analysis of prognostic factors after FSRT in patients with skull base benign meningiomas

Factor	5-year OS (95% CI)	<i>P</i> value	5-year PFS (95% CI)	<i>P</i> value	5-year LCR (95% CI)	<i>P</i> value
Age						
>60 (<i>n</i> = 11)	100	0.429	87.5 (64.6–100)	0.703	100	0.219
≤60 (<i>n</i> = 16)	93.8 (81.8–100)		82.0 (58.1–100)		82.0 (58.1–100)	
Gender						
Female (<i>n</i> = 20)	95.0 (85.4–100)	0.584	94.7 (84.7–100)	0.009	94.7 (84.7–100)	0.04
Male (<i>n</i> = 7)	100		55.6 (7.0–100)		66.7 (13.4–100)	
Gross tumor volume						
<9.1 cc (<i>n</i> = 14)	100	0.28	100	0.022	100	0.044
≥9.1 cc (<i>n</i> = 13)	91.7 (76.0–100)		68.2 (37.2–99.2)		75.8 (45.2–100)	
Planning method						
With MRI fusion (<i>n</i> = 18)	94.1(82.9–100)	0.467	86.5 (69.1–100)	0.229	93.8 (81.8–100)	0.473
Without MRI fusion (<i>n</i> = 9)	100		87.5 (64.6–100)		87.5 (64.6–100)	
Treatment for recurrence						
No (<i>n</i> = 15)	100	0.243	91.7 (76.0–100)	0.102	100	0.013
Yes (<i>n</i> = 12)	90.9 (73.8–100)		68.2 (27.6–100)		68.2 (27.6–100)	
Biological effective dose (Gy) ($\alpha/\beta = 2$)						
≥85 (<i>n</i> = 11)	90.9 (73.8–100)	0.243	60.6 (21.8–99.4)	0.006	68.2 (27.6–100)	0.013
<85 (<i>n</i> = 16)	100		100		100	

OS, overall survival; CI, confidence interval; PFS, progression-free survival; LCR, local control rate; MRI, magnetic resonance imaging.

dose group than the lower dose group, although the difference did not reach the level of statistical significance.

No adverse event was observed in the follow-up period. No optical injury, temporal lobe injury or hydrocephalus, or symptoms related to radiotherapy were observed.

DISCUSSION

The median dose used in the present study is 48–54 Gy with daily dose of 2.0 Gy. It is lower than the dose used in the Heiderberg study (5,7), in which the mean radiation dose

was 56.8 Gy (± 4.4 Gy), and higher than the dose used in the French study (8), in which 45 Gy with daily dose of 1.8 Gy was used. Since a dose–response curve for normal tissues and tumor changes rapidly at the dose range from 40 to 60 Gy with 1.8–2 Gy fractional dose, our results add new biological data for the meningioma and surrounding normal tissue with the long follow-up.

We found that the OS and LCR were 100% at 5 years after FSRT alone for patients with benign skull base meningioma who received FSRT as the initial treatment. This is consistent with a recent article by Korah et al. (6) in which the 8-year LCR was 94% after radiotherapy alone for

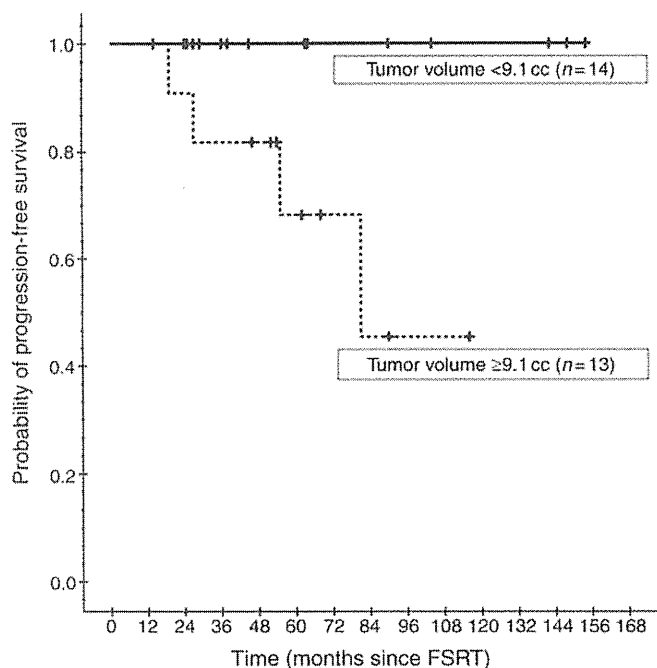


Figure 2. Progression-free survival curves according to the tumor volume. The patients were divided at a median volume of 9.1 cc.

42 patients. Lee et al. (10) also reported a 96.9% LCR at 5 years after SRS alone for 83 patients with cavernous sinus meningiomas. Other series have also suggested a high LCR after radiotherapy alone for benign meningiomas (4,5,11).

After incomplete surgical resection of Simpson's grade III or IV, the recurrence rate of meningiomas is high without radiotherapy (12,13). The recurrence rates for skull base meningioma are especially high, because total resection is much more difficult at this site than at other sites (12,14,15). Adjuvant FSRT immediately after subtotal resection has been suggested to reduce the recurrence rate without lowering the complication rate compared with previous radiotherapy (1,16,17). Previous reports have suggested that radiotherapy for recurrent meningioma is more difficult than radiotherapy used as the initial treatment (14,18). Condra et al. (1) reported that the cause-specific survival was better in patients who received radiotherapy immediately after subtotal resection than those who did not receive radiotherapy. Milker-Zabel et al. (5) also found that patients treated for recurrent meningioma showed a trend toward decreased PFS compared with patients treated with primary therapy, after biopsy or after subtotal resection ($P < 0.06$) in 179 patients with benign or atypical meningiomas.

Our results also suggested that better LCR were obtained for patients who received FSRT with or without surgery as the initial treatment than for those who received FSRT for relapsed tumors. However, the number of patients who were surgically treated and had residual tumor in our institution is uncertain. A small amount of residual benign meningioma after total or subtotal removal often does not enlarge or become symptomatic. Therefore, there is a possible bias that

delayed irradiation was given for a poor prognosis group with a tendency of enlargement and irradiation was not required at all for the majority of patients in a good prognosis group. Precise selection criteria for the early irradiation after surgery are warranted to reduce the unnecessary irradiation for the good prognosis group.

The poorer outcome for recurrent meningioma is likely due to the progressive nature of some meningiomas or a mixed component of atypical meningioma (4,19,20). Meningiomas have been reported to obtain radioresistance or a component of malignant transformation as a natural course of the disease (20–23).

Considering that relapsed meningiomas often contain a progressive component, the treatment policy of applying radiotherapy only in the case of relapsed tumors causes a selection bias in the treatment outcome. The progressive nature of some meningiomas may also result in a leading bias with the treatment policy. Our study showed that the 5-year OS was 96.3% after any initial treatment and 88.2% after FSRT for the same patients' group. We summarized the previous studies of SRS and FSRT in Table 4 and found that our results contained the largest proportion of the relapsed tumors in these series. The tendency for the outcome to be better in the series with a lower proportion of relapsed tumors was not negligible. The lack of these biases may partly explain the excellent results in the group that received radiotherapy alone. The present study suggested that the selection bias and leading bias must be held in mind when we compare the treatment results of radiotherapy among different institutions or compare it with surgical series.

This study showed that the tumor volume was a significant prognostic factor as reported previously (5,22). We summarized the previous studies of SRS and FSRT which discriminated the tumor volume of benign tumors from atypical and malignant meningiomas (Table 4). The median tumor volume was 10 cc less in the majority of studies (4,10,11,24–29). The 5-year PFS and LCR values were more than 90% in these series. This study showed that our results of FSRT for tumors <9.1 cc (median) were as good as those in the previous studies. However, for the total patient group, including patients with larger tumors, the 5-year PFS and LCR were 84.6 and 88.6%, respectively. This finding is consistent with the results of Subach et al., who reported a mean tumor volume of 13.7 cc and a reduction of 5-year LCR to 86% (24).

Conventional 3D-CRT was reported to achieve excellent results in 1980s–early 1990s when CT and MRI images had 5 mm slice thickness and very precise fixation did not make sense. However, in the late 1990s, treatment planning using images with 1–2 mm thickness began to require precise fixation of the skull. Although there is no randomized studies to compare 3D-CRT and FSRT, FSRT can reduce the dose to the critical part of brain tissue with higher certainty than conventional 3D-CRT in the era of 1–2 mm slice thickness of the medical images. There are two recent reviews comparing different radiotherapy techniques such as 3D-CRT, SRS

Table 4. Previous studies of stereotactic radiosurgery and fractionated stereotactic radiotherapy for skull base benign meningioma in which the median or mean tumor volume was described for benign tumors

Institution	SRS or FSRT	No. of patients	Tumor volume median (range) (cc)	Recurrent cases (%)	Follow-up period median (range) (months)	PFS	LCR
Mayo Clinic (30)	SRS	88	10 (2.3–30)	>3 (3%)	35 (12–83)	95.0%	—
University of Pittsburgh (24)	SRS	60	13.7 ^a (0.8–56.8)	>13 (21%)	35 ^a (12–101)	—	86.7%
University of Pittsburgh (10)	SRS	155	6.5 (0.5–52.4)	Unknown	39 ^a (2–145)	—	93.1%
University Hospital, Verona (25)	SRS	111	8.1 ^a (1–20)	0 (0%)	48.2 (12.1–82.5)	96.0%	97.0%
CHU La Timone (4)	SRS	32	2.28 ^a (0.25–60)	2 (6%)	56 ^a (24–118)	100.0%	—
University of Pittsburgh (26)	SRS	219	5.0 (0.47–56.5)	0 (0%)	29 (2–164)	—	93%
Medical University Graz (28)	SRS	200	6.5 (0.38–89.8)	Unknown	94.8 (60–144)	98.5%	—
Seoul National University (11)	SRS	63	6.3 ^a (0.5–18.4)	1 (2%)	77 ^a (48–112)	90.2%	—
University of Pittsburgh (29)	SRS	168	6.1 (0.3–32.5)	35 (21%)	72 (–254)	91.0%	97% (at 10 years)
University of California (27)	FSRT	45	14.5 (1.4–65.66)	8 (31%)	36 (12–53)	97.4% (3 years)	—
Hokkaido University (9.1 cc >)	FSRT	14	4.7 (1.1–9.0)	4 (28.6%)	79.0 (27–154)	100.0%	100.0%
Hokkaido University (all cases)	FSRT	27	9.1 (1.1–86.1)	12 (44.4%)	63.0 (19–154)	84.6%	88.6%

SRS, stereotactic radiosurgery.

^aMean.

and FSRT (30,31). Elia et al. (30) summarized that FSRT has toxicity equivalent to that of SRS, despite its biased use for larger meningiomas with more complicated volumes. Minniti et al. (31) recommended SRS only for tumors <3 cm away more than 3 mm from the optic pathway because of the high risk of long-term neurological deficits.

Selch et al. (27) reported an encouraging 3-year PFS of 97% after FSRT for patients with a median tumor volume of 14.5 cc using a dose fractionation schedule similar to that in our study. Milker-Zabel et al. (5) have published results of FSRT for 179 skull base meningiomas, achieving 90.5 and 89% recurrence-free survival rates for benign meningiomas and atypical meningiomas, respectively, and using a median dose of 57.6 Gy (range: 45–68 Gy). Their results were excellent considering that the median target volume was as large as 33.6 cm³ (1–412.6 cm³) and as many as 141 (44.5%) cases of recurrent disease were included. Eight (4.4%) patients developed new clinical symptoms, such as reduced vision, trigeminal neuralgia and intermittent tinnitus located at the side of the irradiated meningioma after FSRT in their series. The slightly higher dose used in their study might have been the reason for the better tumor control with a little higher complication rate compared with our study. Korah et al. (6) used FSRT, 3D-CRT and SRS for 9, 11 and 22 patients, respectively, and among these, only 1 patient treated with SRS developed a symptomatic radiation-related neurological complication. There were no late adverse reactions in our series (27). Considering that a lower complication rate is an extremely important issue for patients with benign tumors, FSRT is one of the initial treatment options for patients with intracranial skull base meningioma which

locate very close to the critical portion of normal brain tissues.

However, in our relapse cases, the LCR was low. We consider that the 2–3 mm PTV margin was sufficient with our FSRT technique by adding MLC margin to cover the PTV with 90–95% isodose line. However, it is not deniable that the high relapse rate of the larger tumors may also be explained by the small PTV margins used in our study. Goldsmith et al. (32) reported that the PFS rate in the group treated with a minimum tumor dose of >52 Gy was better than the group treated with ≤52 Gy (93 vs. 65%; *P* = 0.04). When FSRT was used for treating the case of the tumor located near the organ at risk (OAR), we must have reduced the margin for PTV to exclude the OAR from the high-dose area. Thus, the dose concentration for the tumor was gotten worse than an ideal dose distribution. Intensity-modulated radiotherapy (IMRT) is expected to increase the therapeutic ratio by reducing the dose to normal tissue because IMRT can deliver the prescription dose to the targets without worsen the dose concentration. For improvement of the LCR of those relapse cases, IMRT with a fractionated schedule will be more appropriate than simple FSRT to increase the dose for these tumors without increasing the dose to the surrounding normal tissue (33–36). However, higher radiation dose to the rest of the body and higher cost to the patient must be taken into account for each patient to use IMRT.

In conclusion, the long-term outcome suggests that FSRT is a safe and effective treatment for intracranial skull base benign meningioma, especially for those who have tumors <9.1 cc or would receive FSRT with or without surgery as the initial treatment.

Funding

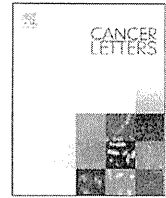
This study was partly supported by Grant-in-Aid for Scientific Research (no. 21249065) from Ministry of Education, Culture, Sports, Science and Technology, Japan, and a part of this study was presented in the poster session of 51th Annual Meeting of ASTRO in Chicago (USA), 1–5 November 2009.

Conflict of interest statement

None declared.

References

- Condra KS, Buatti JM, Mendenhall WM, Friedman WA, Marcus RB, Jr, Rhoton AL. Benign meningiomas: primary treatment selection affects survival. *Int J Radiat Oncol Biol Phys* 1997;39:427–36.
- Whittle IR, Smith C, Navoo P, Collie D. Meningiomas. *Lancet* 2004;363:1535–43.
- Kondziolka D, Flickinger JC, Perez B. Judicious resection and/or radiosurgery for parasagittal meningiomas: outcomes from a multicenter review. Gamma Knife Meningioma Study Group. *Neurosurgery* 1998;43:405–13; discussion 13–4.
- Roche PH, Pellet W, Fuentes S, Thomassin JM, Regis J. Gamma knife radiosurgical management of petroclival meningiomas results and indications. *Acta Neurochir (Wien)* 2003;145:883–8; discussion 8.
- Milker-Zabel S, Zabel A, Schulz-Ertner D, Schlegel W, Wannenmacher M, Debus J. Fractionated stereotactic radiotherapy in patients with benign or atypical intracranial meningioma: long-term experience and prognostic factors. *Int J Radiat Oncol Biol Phys* 2005;61:809–16.
- Korah MP, Nowlan AW, Johnstone PA, Crocker IR. Radiation therapy alone for imaging-defined meningiomas. *Int J Radiat Oncol Biol Phys* 2010;76:181–6.
- Milker-Zabel S, Zabel-du Bois A, Huber P, Schlegel W, Debus J. Fractionated stereotactic radiation therapy in the management of benign cavernous sinus meningiomas: long-term experience and review of the literature. *Strahlenther Onkol* 2006;182:635–40.
- Litre CF, Colin P, Noudel R, Peruzzi P, Bazin A, Sherpereel B, et al. Fractionated stereotactic radiotherapy treatment of cavernous sinus meningiomas: a study of 100 cases. *Int J Radiat Oncol Biol Phys* 2009;74:1012–7.
- Simpson D. The recurrence of intracranial meningiomas after surgical treatment. *J Neurol Neurosurg Psychiatry* 1957;20:22–39.
- Lee JY, Niranjan A, McInerney J, Kondziolka D, Flickinger JC, Lunsford LD. Stereotactic radiosurgery providing long-term tumor control of cavernous sinus meningiomas. *J Neurosurg* 2002;97:65–72.
- Han JH, Kim DG, Chung HT, Park CK, Paek SH, Kim CY, et al. Gamma knife radiosurgery for skull base meningiomas: long-term radiologic and clinical outcome. *Int J Radiat Oncol Biol Phys* 2008;72:1324–32.
- De Jesus O, Sekhar LN, Parikh HK, Wright DC, Wagner DP. Long-term follow-up of patients with meningiomas involving the cavernous sinus: recurrence, progression, and quality of life. *Neurosurgery* 1996;39:915–9; discussion 9–20.
- Mathiesen T, Lindquist C, Kihlstrom L, Karlsson B. Recurrence of cranial base meningiomas. *Neurosurgery* 1996;39:2–7; discussion 8–9.
- Maroon JC, Kennerdell JS, Vidovich DV, Abela A, Sternau L. Recurrent sphenoid-orbital meningioma. *J Neurosurg* 1994;80:202–8.
- Black PM, Villavicencio AT, Rhoads C, Loeffler JS. Aggressive surgery and focal radiation in the management of meningiomas of the skull base: preservation of function with maintenance of local control. *Acta Neurochir (Wien)* 2001;143:555–62.
- Debus J, Wuendrich M, Pirzkall A, Hoess A, Schlegel W, Zuna I, et al. High efficacy of fractionated stereotactic radiotherapy of large base-of-skull meningiomas: long-term results. *J Clin Oncol* 2001;19:3547–53.
- Mendenhall WM, Morris CG, Amdur RJ, Foote KD, Friedman WA. Radiotherapy alone or after subtotal resection for benign skull base meningiomas. *Cancer* 2003;98:1473–82.
- Al-Mefty O, Kadri P, Pravdenkova S, Sawyer JR, Stangeby C, Husain M. Malignant progression in meningioma: documentation of a series and analysis of cytogenetic findings. *J Neurosurg* 2004;101:210–8.
- Aghi MK, Carter BS, Cosgrove GR, Ojemann RG, Amin-Hanjani S, Martuza RL, et al. Long-term recurrence rates of atypical meningiomas after gross total resection with or without postoperative adjuvant radiation. *Neurosurgery* 2009;64:56–60.
- Ohba S, Yoshida K, Hirose Y, Ikeda E, Kawase T. Early malignant transformation of a petroclival meningotheial meningioma. *Neurosurg Rev* 2009;32:495–9.
- Colvett KT, Hsu DW, Su M, Lingood RM, Pardo FS. High PCNA index in meningiomas resistant to radiation therapy. *Int J Radiat Oncol Biol Phys* 1997;38:463–8.
- Maillo A, Orfao A, Espinosa AB, Sayagues JM, Merino M, Sousa P, et al. Early recurrences in histologically benign/grade I meningiomas are associated with large tumors and coexistence of monosomy 14 and del(1p36) in the ancestral tumor cell clone. *Neuro Oncol* 2007;9:438–46.
- Nakane Y, Natsume A, Wakabayashi T, Oi S, Ito M, Inao S, et al. Malignant transformation-related genes in meningiomas: allelic loss on 1p36 and methylation status of p73 and RASSF1A. *J Neurosurg* 2007;107:398–404.
- Subach BR, Lunsford LD, Kondziolka D, Maitz AH, Flickinger JC. Management of petroclival meningiomas by stereotactic radiosurgery. *Neurosurgery* 1998;42:437–43; discussion 43–5.
- Nicolato A, Foroni R, Alessandrini F, Maluta S, Bricolo A, Gerosa M. The role of Gamma Knife radiosurgery in the management of cavernous sinus meningiomas. *Int J Radiat Oncol Biol Phys* 2002;53:992–1000.
- Flickinger JC, Kondziolka D, Maitz AH, Lunsford LD. Gamma knife radiosurgery of imaging-diagnosed intracranial meningioma. *Int J Radiat Oncol Biol Phys* 2003;56:801–6.
- Selch MT, Ahn E, Laskari A, Lee SP, Agazaryan N, Solberg TD, et al. Stereotactic radiotherapy for treatment of cavernous sinus meningiomas. *Int J Radiat Oncol Biol Phys* 2004;59:101–11.
- Kreil W, Luggin J, Fuchs I, Weigl V, Eustacchio S, Papaefthymiou G. Long term experience of gamma knife radiosurgery for benign skull base meningiomas. *J Neurol Neurosurg Psychiatry* 2005;76:1425–30.
- Flannery TJ, Kano H, Lunsford LD, Sirin S, Tormenti M, Niranjan A, et al. Long-term control of petroclival meningiomas through radiosurgery. *J Neurosurg* 2010;112:957–64.
- Elia AEH, Shih HA, Loeffler JS. Stereotactic radiation treatment for benign meningiomas. *Neurosurg Focus* 2007;23:E5.
- Minniti G, Amichetti M, Enrici RM. Radiotherapy and radiosurgery for benign skull base meningiomas. *Radiat Oncol* 2009;4:42.
- Goldsmith BJ, Wara WM, Wilson CB, Larson DA. Postoperative irradiation for subtotally resected meningiomas. A retrospective analysis of 140 patients treated from 1967 to 1990. *J Neurosurg* 1994;80:195–201.
- Khoo VS, Oldham M, Adams EJ, Bedford JL, Webb S, Brada M. Comparison of intensity-modulated tomotherapy with stereotactically guided conformal radiotherapy for brain tumors. *Int J Radiat Oncol Biol Phys* 1999;45:415–25.
- Pirzkall A, Carol M, Lohr F, Hoss A, Wannenmacher M, Debus J. Comparison of intensity-modulated radiotherapy with conventional conformal radiotherapy for complex-shaped tumors. *Int J Radiat Oncol Biol Phys* 2000;48:1371–80.
- Pirzkall A, Debus J, Haering P, Rhein B, Grosser KH, Hoss A, et al. Intensity modulated radiotherapy (IMRT) for recurrent, residual, or untreated skull-base meningiomas: preliminary clinical experience. *Int J Radiat Oncol Biol Phys* 2003;55:362–72.
- Milker-Zabel S, Zabel-du Bois A, Huber P, Schlegel W, Debus J. Intensity-modulated radiotherapy for complex-shaped meningioma of the skull base: long-term experience of a single institution. *Int J Radiat Oncol Biol Phys* 2007;68:858–63.



Local convection-enhanced delivery of chemotherapeutic agent transiently opens blood–brain barrier and improves efficacy of systemic chemotherapy in intracranial xenograft tumor model

Taigen Nakamura, Ryuta Saito*, Shin-ichiro Sugiyama, Yukihiro Sonoda, Toshihiro Kumabe, Teiji Tominaga

Department of Neurosurgery, Tohoku University Graduate School of Medicine, Sendai, Miyagi, Japan

ARTICLE INFO

Article history:

Received 15 February 2011

Received in revised form 2 June 2011

Accepted 12 June 2011

Keywords:

Convection-enhanced delivery

Local chemotherapy

Blood–brain barrier

Brain tumor

ACNU

ABSTRACT

Recently, local chemotherapy proved its efficacy against malignant gliomas. Under the hypothesis that local delivery of chemotherapeutic agents into the brain parenchyma induce opening of the blood–brain barrier (BBB), we evaluated the opening of BBB after convection-enhanced delivery of nimustine hydrochloride into the brain parenchyma. Local convection-enhanced delivery of nimustine hydrochloride transiently opened the BBB from about 7–12 days after delivery in normal rodent brain. Systemic chemotherapy during this period of BBB disruption had synergistic effects resulting in prolonged survival of tumor-bearing rats. The present strategy may provide a new approach for glioma chemotherapy.

© 2011 Elsevier Ireland Ltd. All rights reserved.

1. Introduction

Glioblastoma is the most common and most aggressive type of primary brain tumor. Approximately 3 in 100,000 people in the US and European countries are diagnosed with glioblastoma every year, and the median survival of a patient with glioblastoma is 15 months [1]. Only a minority of patients live longer than 3 years because therapies for the treatment of glioblastoma have only limited effectiveness despite the best efforts of researchers [2]. Post-surgical placement of small biodegradable polymer wafers designed to deliver carmustine (BCNU) directly into the resection cavity provides a survival benefit in patients with newly diagnosed and recurrent glioblastoma [3,4]. This procedure illustrates the therapeutic potential of extensive local chemotherapy against this devastating disease.

The emergence of effective cancer chemotherapy is one of the major medical advances of the second half of the 20th century [5]. New lineups of chemotherapeutic agents and molecular targeted agents have been introduced to treat neoplasms. However, patients with gliomas fail to receive the benefits provided by most of these agents. Temozolomide is the only agent that has demonstrated therapeutic efficacy [6]. The properties of the blood–brain barrier (BBB), although compromised to some extent in glioblastomas, may be the reason for this failure [7]. Poor penetration of most anticancer drugs across the BBB and into the central nervous system is well documented. Even drugs that penetrate the BBB cannot reach adequate drug concentrations in brain-tumor tissue without causing systemic side effects [7]. Therefore, methods to transiently open this barrier have been extensively studied, including osmotic disruption using hyperosmotic shock [8], and biochemical disruption by administration of vasoactive substances [9].

Local drug delivery to the affected brain location should theoretically bypass the BBB, reduce systemic drug levels to minimize the side effects of chemotherapy, and provide

* Corresponding author. Address: Department of Neurosurgery, Tohoku University Graduate School of Medicine, 1-1 Seiryō-machi, Aoba-ku, Sendai, Miyagi 980-8574, Japan. Tel.: +81 22 717 7230; fax: +81 22 717 7233.

E-mail address: ryuta@nsg.med.tohoku.ac.jp (R. Saito).

prolonged higher levels of intracerebral chemotherapeutic agents relative to those obtainable by systemic administration [7,10]. However, for many local drug-delivery technologies including simple intratumoral injection or polymer implantation, the ultimate efficacy depends on the diffusion of the drugs into the brain parenchyma. An important advance in local drug delivery is the development of convection-enhanced delivery (CED) [11]. This technique uses bulk flow to directly deliver small or large molecules to targeted sites in clinically significant volumes of tissue, resulting in improved volumes of distribution compared with simple diffusion techniques [10]. This technique is now being applied to deliver BCNU [12], topotecan [13], carboplatin, gemcitabine [14], and paclitaxel [15] to brain tumors, all with promising outcomes.

Recently, we have been investigating the CED of nimustine hydrochloride (ACNU) as a new strategy to effectively treat glioblastoma [16–18]. During our study, we observed a period when the brain treated with ACNU becomes enhanced on magnetic resonance imaging after intravenous administration of contrast agents, suggesting that the BBB becomes leaky after local administration of chemotherapeutic agent. In the present study, we tried to identify this leaky period, and investigated whether the efficacy of combination systemic chemotherapy was enhanced during this period.

2. Materials and methods

2.1. Pegylated (polyethylene glycol-coated) liposomal doxorubicin (PLD) and ACNU

PLD (Doxil; Alza Pharmaceuticals, Mountain View, CA) was obtained commercially. The commercial PLD solution contained 2 mg/mL of doxorubicin. ACNU was provided by Daiichi-Sankyo Co. Ltd. (Tokyo, Japan). Infusion solutions of ACNU were prepared by diluting ACNU in 0.9% NaCl solution to a concentration of 1 mg/mL.

2.2. Tumor cell line, animals, and intracranial xenograft technique

The 9 L rat gliosarcoma cells (American Type Culture Collection, Rockville, MD) were maintained as monolayers in a complete medium consisting of Eagle's minimal essential medium supplemented with 10% fetal bovine serum, non-essential amino acids, and 100 U/mL penicillin G. Cells were cultured at 37 °C in a humidified atmosphere consisting of 95% air and 5% CO₂. Male Sprague–Dawley rats weighting approximately 200 g were purchased from Charles-River Japan Laboratories (Tsukuba, Ibaraki, Japan). Male Fisher 344 rats weighting approximately 200 g were purchased from Kumagai-Shigeyasu Co., Ltd. (Sendai, Miyagi, Japan). All protocols used for the animal studies were approved by the Institute for Animal Experimentation of Tohoku University Graduate School of Medicine. To establish the intracranial xenograft tumor model, cells were harvested by trypsinization, washed once with Hanks' balanced salt solution without Ca²⁺ and Mg²⁺ (HBSS), and resuspended in HBSS for implantation. A cell

suspension containing 5×10^5 cells/10 μ L HBSS was used for implantation into the striatal region of the Fisher 344 rat brains. Under deep halothane anesthesia, rats were placed in a small-animal stereotactic frame (David Kopf Instrument, Tujunga, CA). A sagittal incision was made to expose the cranium followed by a burr hole in the skull located at 0.5 mm anterior and 3 mm lateral from the bregma using a small dental drill. Cell suspension (5 μ L) was injected over 2 min at a depth of 4.5 mm from the brain surface; after a 2-min wait, another 5 μ L was injected over 2 min at a depth of 4.0 mm; and after a final 2-min wait, the needle was removed and the wound was sutured.

2.3. Convection-enhanced delivery

CED with a volume of 20 μ L of ACNU or PBS was performed as described previously [19,20]. Briefly, the infusion system consisted of a reflux-free, step-design infusion cannula connected to a loading line (containing ACNU or PBS (GIBCO™ PBS; Life technologies Japan Ltd., Tokyo, Japan)) and an olive oil infusion line. A 1-mL syringe (filled with oil) mounted onto a micro-infusion pump (BeeHive; Bioanalytical Systems, West Lafayette, IN) regulated the flow of fluid through the system. Based on chosen coordinates, the infusion cannula was mounted onto stereotactic holders and guided to the target region of the brain through burr holes made in the skull. The following ascending infusion rates were applied to achieve 20 μ L infusion: 0.2 μ L/min (15 min) + 0.5 μ L/min (10 min) + 0.8 μ L/min (15 min).

2.4. Evaluation of toxicity

Three healthy male Sprague–Dawley rats weighing approximately 200 g received a single 20 μ L CED infusion of 1 mg/mL ACNU. Rats were monitored daily for survival, weekly weights, and general health. Rats were euthanized on the 60th day after the CED, and their brains were removed, fixed, subjected to paraffin sectioning (5 μ m), and stained with hematoxylin and eosin.

2.5. Volumetric evaluation of BBB disruption

Twenty normal male Fisher 344 rats weighting approximately 200 g received a single 20 μ L CED infusion of 1 mg/mL ACNU and were randomly assigned to five groups. In each group of four rats, 1 mL of 2% Evans blue solution (Sigma–Aldrich, Tokyo, Japan) in saline was administered through the tail veins at 3, 7, 12, 20, and 30 days after CED. Rats were euthanized 30 min after administration. After transcardial perfusion with NaCl solution, their brains were harvested, frozen with ice-cold isopentane, and cut into serial coronal sections (25 μ m) with a cryostat. Evans blue generates fluorescence under UV illumination, so the areas of brain section containing extravasated Evans blue were visualized using a fluorescence microscope, and a charged-coupled device camera with a fixed aperture was used to capture the image. The volumes of brain that contained extravasated Evans blue were calculated from these images.

2.6. Quantitative evaluation of BBB disruption

Twenty-four normal male Fisher 344 rats weighing approximately 200 g received a single 20 μ L CED infusion of 1 mg/mL ACNU. As for volumetric analysis, 1 mL of 4% Evans blue solution was administered to Fisher 344 rats 3 ($n = 9$), 7 ($n = 9$), and 30 ($n = 6$) days after CED. Rats were euthanized 30 min after Evans blue administration. After transcardial perfusion with NaCl solution, their brains were harvested. Extravasation of Evans blue in the hemispheres (3 mm anterior and 3 mm posterior from the CED point) was measured according to the method of Chan et al. [21,22]. After homogenization with 1 mL PBS, samples were centrifuged at 1000g for 30 min. Supernatants (0.7 mL) were taken, and an equal volume of 100% trichloroacetic acid was added to precipitate protein. The samples were allowed to stand overnight at 4 °C, and were then centrifuged at 1000g for 30 min. The absorbance of Evans blue at 610 nm was measured in the supernatants using a spectrophotometer. Evans blue content was expressed as μ g per hemisphere calculated against a standard.

2.7. Extravasation of PLD after CED in intracranial xenograft tumor model

Six male Fisher 344 rats with intracranial xenograft tumors were used for this study. Five days after tumor implantation, three rats received CED of ACNU (0.1 mg/mL, 20 μ L), and three rats received CED of 20 μ L PBS. Seven days after CED, all rats received bolus intravenous injections of 1 mL PLD solution (2.0 mg/mL) via the tail veins. Thirty minutes after PLD administration, rats were perfused transcardially with NaCl solution. Brains were harvested and frozen with ice-cold isopentane, and cut into serial coronal sections (25 μ m) with a cryostat. PLD generates fluorescence under UV illumination, so the areas of brain section containing extravasated PLD were visualized using a fluorescence microscope, and a charged-coupled device camera with a fixed aperture was used to capture the image. The same sections were then stained with hematoxylin and eosin.

2.8. Survival study using the intracranial xenograft model

Forty-two male Fisher 344 rats with intracranial xenograft tumors were randomly assigned to five groups as summarized in Table 1: (a) control group received CED of PBS ($n = 9$), (b) group received intravenous PLD administration after CED of PBS ($n = 9$), (c) group received CED of ACNU ($n = 8$), (d) group received intravenous PLD adminis-

tration after CED of ACNU ($n = 9$); and (e) group received CED of ACNU after intravenous PLD administration ($n = 7$). Five days after tumor cell implantation (Day 5), single CED infusions (20 μ L infusion of 1 mg/mL ACNU or PBS) were performed for groups (a, b, c, and d), and bolus intravenous injections of 400 μ L PLD (2.0 mg/mL) via the tail veins were performed for group (e). Seven days later (Day 12), bolus intravenous injections of 400 μ L PLD (2.0 mg/mL) via the tail veins were performed for groups (b, d, and e). Six days later (Day 18), bolus intravenous injections of 400 μ L PLD (2.0 mg/mL) via the tail veins were performed for groups (b and d), and CED infusions (20 μ L of 1 mg/mL ACNU) were performed for group (e). The dose of PLD used in this study was selected based on previous studies [23,24]. Survival was expressed as a Kaplan–Meier curve. Survival was compared between the treatment groups with a log-rank test.

3. Results

3.1. Negligible local toxicity of 1 mg/mL ACNU delivered via CED

CED infusion of 20 μ L ACNU at concentration of 1 mg/mL caused little local tissue damage when infused into normal rat hemisphere (Fig. 1), as previously reported [16,17]. Slight tissue damage was noted only at the needle tract without obvious tissue damage in the surrounding brain that received ACNU. Even at higher magnification, no strong inflammatory response or tissue necrosis was detected. No rat developed neurological deficit or lost their weight. This dose of ACNU (20 μ L of 1 mg/mL ACNU) was used throughout this study.

3.2. Extravasation of intravenous Evans blue 7 days after CED of ACNU

Although CED of ACNU caused little local tissue change as described above, leakage of intravenously infused 2% Evans blue solution was observed 7 days after CED of ACNU into the hemispheres of normal Fisher 344 rats. Representative brain sections are shown in Fig. 2A. Fluorescent microscopy detected Evans blue in the brain parenchyma indicating leakage from the BBB. In contrast, leakage of Evans blue was hardly observed 7 days after CED of PBS (Fig. 2B). Results were similar for all four rats tested.

3.3. Transient disruption of BBB after CED of ACNU

To test the time course of BBB disruption, leakage of intravenously infused Evans blue solution was evaluated 3, 7, 12, 20, and 30 days after CED of ACNU using fluorescent images. The leakage of Evans blue was small 3 days after CED, but became prominent from 7 to 12 days after CED, and then diminished (Fig. 3). Volumetric analysis of the fluorescent area confirmed the findings.

3.4. Quantitative analysis of transient disruption of BBB after CED of ACNU

Quantitative spectrophotometric analysis of Evans blue leakage through the disrupted BBB compared the amount of Evans blue in the brains of rats 3, 7, and 30 days after CED of ACNU. Brains of rats contained

Table 1
Five groups for survival study using the intracranial xenograft model.

Group	<i>n</i>	Day 0	Day 5	Day 12	Day 18
(a) Control	9	Implantation	PBS CED	PBS iv	PBS iv
(b) PLD iv	9	Implantation	PBS CED	PLD iv	PLD iv
(c) ACNU CED	8	Implantation	ACNU CED	PBS iv	PBS iv
(d) ACNU CED + PLD iv	9	Implantation	ACNU CED	PLD iv	PLD iv
(e) PLD iv + ACNU CED	7	Implantation	PLD iv	PLD iv	ACNU CED

Abbreviations: iv = intravenous, CED = convection-enhanced delivery, PLD = pegylated liposomal doxorubicin, PBS = phosphate buffered saline.

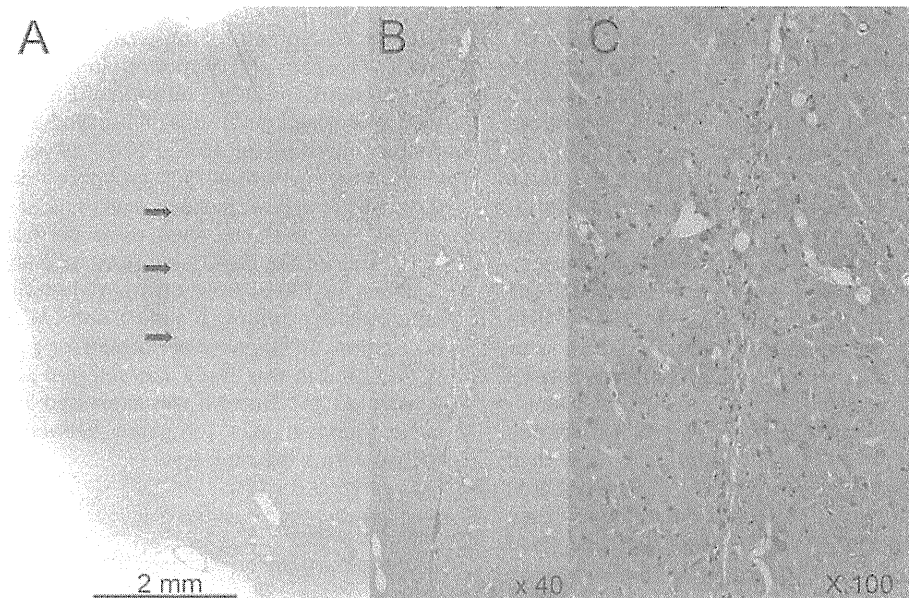


Fig. 1. Local tissue toxicity of ACNU administered via CED in the normal adult rat brain. Rat brains were treated with a single CED infusion of 20 μ L of 1.0 mg/mL ACNU. Representative hematoxylin and eosin sections from rats euthanized 30 days after CED. Rats showed no drug-induced damage (A). Arrows indicate the needle tract. Higher magnification of tissue around needle tract (B: $\times 40$, C: $\times 100$).

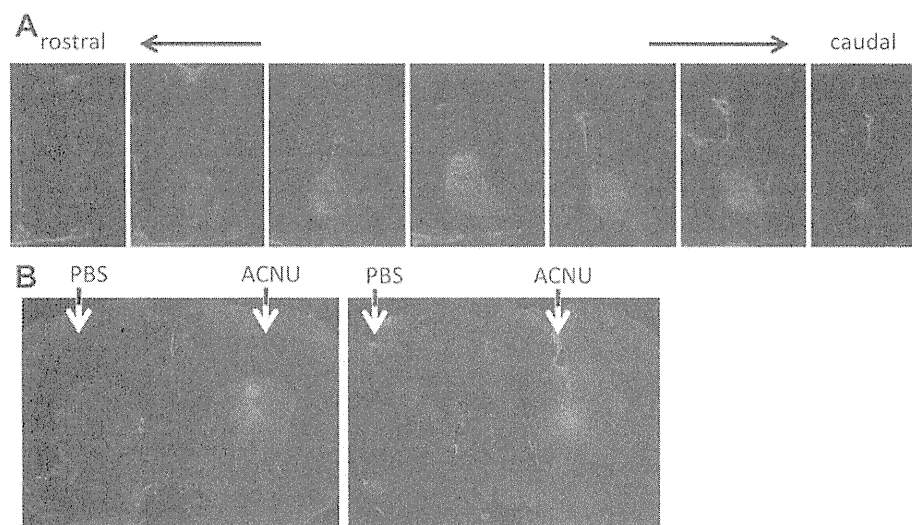


Fig. 2. Seven days after CED of ACNU into the hemisphere of normal Fisher 344 rats, 2% Evans blue solution was injected via the tail vein. Rats were euthanized 30 min after Evans blue administration. After transcardial perfusion with NaCl solution, their brains were harvested, frozen, and cut into serial coronal sections (25 μ m) with a cryostat. Brain sections were observed with a fluorescence microscope to detect the extravasation of Evans blue. Sequential brain sections at 500- μ m intervals from a representative rat are shown (A). Sequential brain sections at 500- μ m intervals of another rat that received tail vein injection of 2% Evans blue 7 days after CED of ACNU into one hemisphere and CED of PBS into the other hemisphere (B).

significantly higher amount of Evans blue 7 days after CED than on other days (Fig. 4), which confirmed the findings of the volumetric analysis.

3.5. Disruption of BBB after CED of ACNU in xenograft tumor model

Tumor vessels are usually more leaky than normal vessels. BBB disruption was evaluated in the intracranial xenograft tumor model. Seven days after CED of ACNU ($n = 3$) or PBS ($n = 3$), PLD was injected from the tail vein. Although mild leakage was observed in rats that received CED of PBS, leakage was more extensive in rats that received CED of ACNU (Fig. 5). One of three rats that received CED of ACNU harbored two separate tumors located just at the needle tract of ACNU infusion and at a dee-

per location probably not reached by infused ACNU. This enabled us to evaluate the efficacy of infused ACNU. Leakage of PLD was more prominent in the tumor located at the needle tract compared to the deeply located tumor. With the hypothesis that this leakage of PLD after CED of ACNU may benefit the survival of brain tumor xenografts, we conducted the following survival study.

3.6. Survival study

Survival study is summarized as a Kaplan–Meier curve (Fig. 6). CED of ACNU ($P = 0.017$; log-rank test) but not PLD ($P = 0.26$) prolonged the survival of tumor-bearing rats. Survival was improved when CED of ACNU

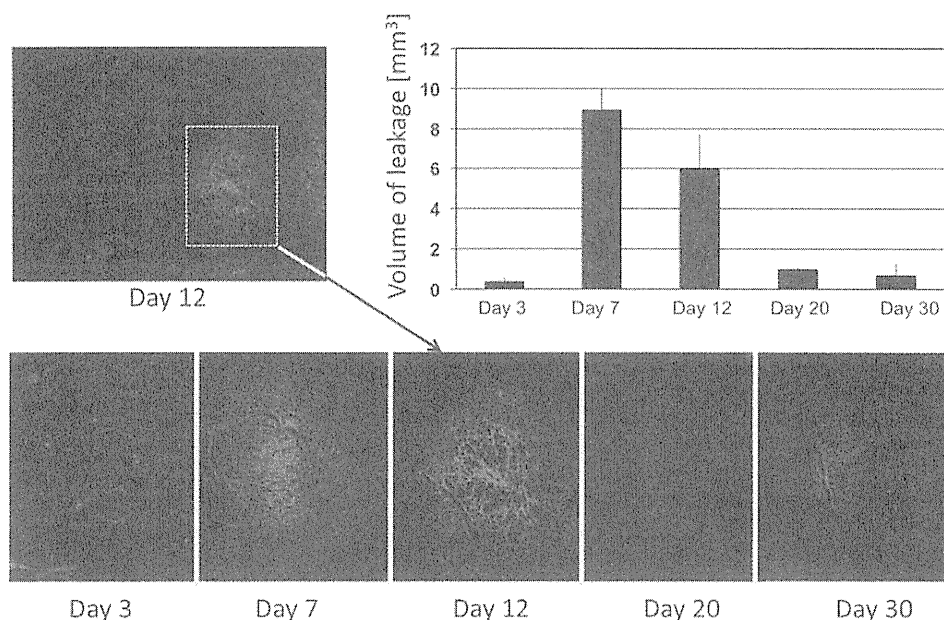


Fig. 3. Leakage of intravenously infused Evans blue solution 3, 7, 12, 20, and 30 days after CED of ACNU. Brains were processed as in Fig. 2 and observed under a fluorescence microscope. Representative image from rat brain that received Evans blue 12 days after CED (upper left). Lower images depict the magnified images of the boxed area from each day period. The fluorescence images were acquired under the same conditions. Volumetric analysis of the area that contained fluorescence from Evans blue (upper right). Bars at top of each column indicate the standard deviation.

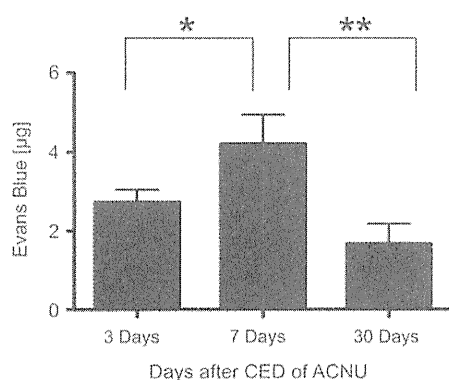


Fig. 4. Evans blue content in the brains of rats that received intravenous injection of 4% Evans blue solution 3, 7, and 30 days after CED of ACNU was measured using a spectrophotometer. Evans blue content was expressed as µg per hemisphere calculated against a standard. Bars at top of each column indicate the standard deviation. * $P = 0.042$, ** $P = 0.013$, Student t -test.

was given prior to PLD ($P = 0.0001$; compared with control, $P = 0.003$; compared with CED of ACNU alone), but not when PLD was given prior to CED of ACNU ($P = 0.27$; compared with control). BBB disruption caused by CED of ACNU may be one reason for this improved survival.

4. Discussion

Our previous studies reported the safety and efficacy of CED of ACNU in the intracranial xenograft tumor model [16,17]. The present study confirmed that CED of 1 mg/mL ACNU produced no severe toxicity (Fig. 1). However, disruption of the BBB was observed. Qualitative eval-

uation revealed robust distribution of Evans blue in the normal rat hemisphere after intravenous administration, which was confirmed by quantitative evaluation.

Local chemotherapy can be effective against malignant gliomas, and CED can deliver drugs much more extensively into the target region, but may have some limitations. The vast majority of neoplastic cells in malignant gliomas are found within the tumor bed and within 2 cm of the enhanced borders, but migrating cells can be found several centimeters away from the tumor and even in the contralateral hemisphere [25]. Moreover, dissemination limits the survival of patients with locally well controlled malignant gliomas [26]. Therefore, effective local therapy should be administered together with effective systemic therapy. However, systemic chemotherapy is limited because 98% of small molecules and 100% of large molecules cannot cross the BBB [27]. Many promising agents including molecular targeted agents have not been as effective as expected.

In this context, our findings provide the rationale for combining local and systemic chemotherapy. The observed BBB disruption after local chemotherapy was reversible. Leakage was observed only between 1 and 2 weeks after delivery of ACNU. The exact mechanism for this transient disruption of the BBB is not clear, but slight disturbance of the BBB caused by chemotherapeutic agents is likely to recover fairly rapidly. In this study, delivery of intravenous Evans blue or PLD was augmented during this time window, but not later. Therefore, this transient dysfunction of the BBB gives a time window for effective delivery of systemic chemotherapeutic agents.

Drug delivery to brain tumors has been a controversial subject. Some researchers believe that the BBB is not

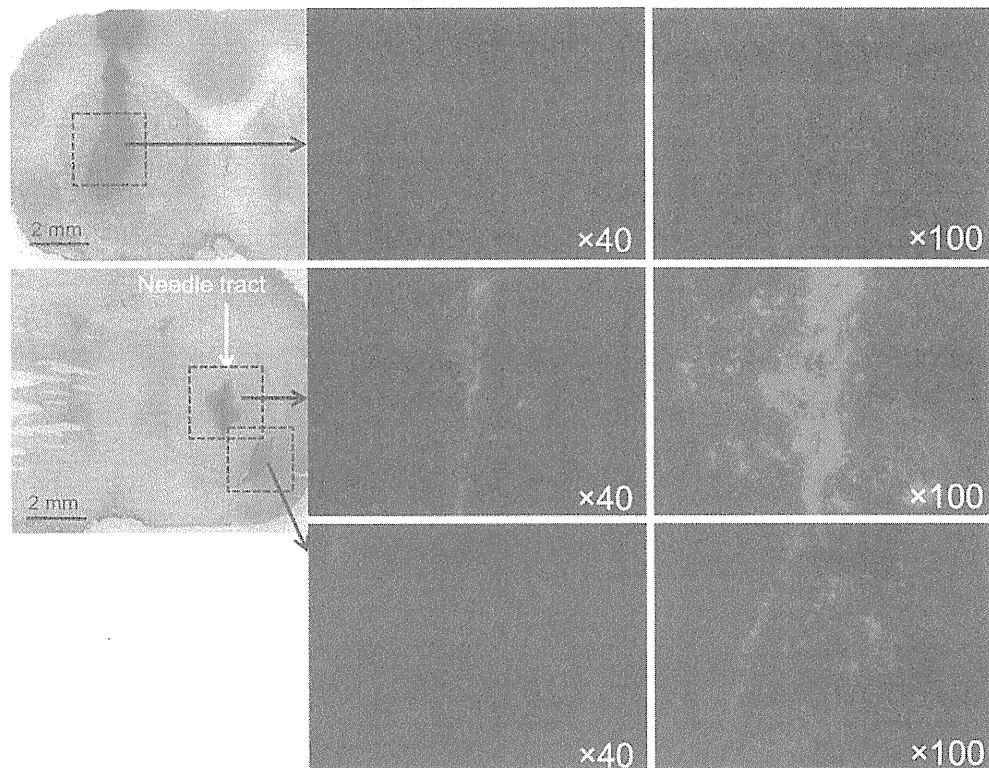


Fig. 5. Seven days after CED of ACNU ($n = 3$) or PBS ($n = 3$), PLD was injected via the tail vein. Although mild leakage was observed in rats that received CED of PBS (upper row), leakage was more extensive in rats that received CED of ACNU (middle and lower row). One of three rats that received CED of ACNU had two separate tumors, located just at the needle tract of ACNU infusion and at a deeper location probably not reached by infused ACNU. Leakage of PLD was more prominent in the tumor located at the needle tract (middle row) compared to the deeply located tumor (lower row).

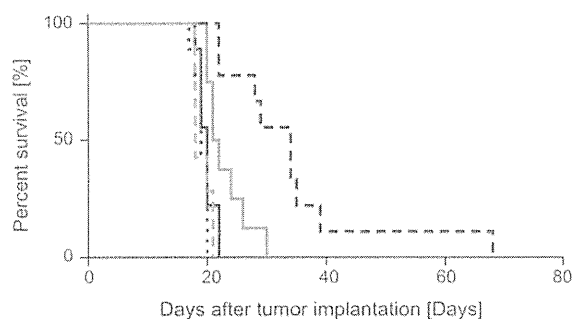


Fig. 6. Survival of the five groups expressed as a Kaplan–Meier curve. Black solid line, (a) control; black dotted line, (b) intravenous PLD; gray solid line, (c) CED of ACNU; black dashed line, (d) CED of ACNU plus intravenous PLD; and gray dashed line, (e) intravenous PLD plus CED of ACNU.

important, while others believe it is the major obstacle in treatment [28]. However, on the whole, the understanding is that the BBB and the blood–tumor barrier prevent drugs from reaching brain tumors in sufficient concentrations to kill the tumor cells [7]. In this study, we evaluated the leakage of PLD into the xenograft brain tumor model. Permeability of experimental gliomas is reported to be 10^4 – 10^5 higher than the normal brain if the molecular size of the agent is small enough [29]. Fluorescence from PLD was

observed in the tumors, but the fluorescence was obviously more intense after infusion of ACNU. The survival study also demonstrated the efficacy of the combination of ACNU CED and intravenous PLD, but only if intravenous PLD was given during the period of BBB disruption. This combination significantly prolonged survival of the tumor model rats if intravenous PLD was given 5 and 12 days after CED of ACNU. This efficacy was not observed if the agents were used in the opposite order. Moreover, the group treated by CED of ACNU following intravenous administration of PLD did not survive longer than the control group while the group treated by CED of ACNU had significantly longer survival than the control group. This may be because that xenografted tumors 18 days after implantation become too large to be treated by CED of 20 μ L ACNU although intravenous PLD was given 5 and 12 days after implantation.

Many methods have been assessed to transiently disrupt the BBB for effective drug delivery to the central nervous system. Osmotic disruption such as hyperosmotic shock, and biochemical disruption induced by administration of vasoactive substances have been tested [8,9,27]. Tumor chemotherapy combined with these BBB opening agents seemed promising at first, but were abandoned because of the potential for structural brain damage in areas of BBB disruption. Compared with these strategies, the present method disrupts the BBB only at the site of drug

distribution achieved by CED. As the CED of chemotherapeutic agents targets the site of tumor invasion, this method may be effective without severe toxicity to other parts of the brain.

The present study showed that local application of chemotherapeutic agents into the brain parenchyma induced transient opening of the BBB. Systemic chemotherapy during this period of BBB disruption had synergistic effects resulting in prolonged survival of tumor-bearing rats. The present strategy may provide a new approach for glioma chemotherapy.

Conflict of interest

None declared.

Acknowledgements

This work was supported in part by Grants-in-Aid for Scientific Research from the Ministry of Health, Labour and Welfare in Japan to R.S. (Grant No. 21791341, 2009).

References

- [1] A. Jemal, T. Murray, A. Samuels, A. Ghafoor, E. Ward, M.J. Thun, Cancer statistics 2003, *CA Cancer J. Clin.* 53 (2003) 5–26.
- [2] A.A. Brandes, State-of-the-art treatment of high-grade brain tumors, *Semin. Oncol.* 30 (6 Suppl. 19) (2003) 4–9.
- [3] S. Gururangan, L. Cokgor, J.N. Rich, S. Edwards, M.L. Affronti, J.A. Quinn, J.E. Herndon 2nd, J.M. Provenzale, R.E. McLendon, S. Tourt-Uhlig, J.H. Sampson, V. Stafford-Fox, S. Zaknoen, M. Early, A.H. Friedman, H.S. Friedman, Phase I study of Gliadel wafers plus temozolomide in adults with recurrent supratentorial high-grade gliomas, *Neurol. Oncol.* 3 (2001) 246–250.
- [4] M. Westphal, D.C. Hilt, E. Bortey, P. Delavault, R. Olivares, P.C. Warnke, I.R. Whittle, J. Jääskeläinen, Z. Ram, A phase 3 trial of local chemotherapy with biodegradable carmustine (BCNU) wafers (Gliadel wafers) in patients with primary malignant glioma, *Neurol. Oncol.* 5 (2003) 79–88.
- [5] M.R. Green, Targeting targeted therapy, *New Engl. J. Med.* 350 (2004) 2191–2193.
- [6] R. Stupp, W.P. Mason, M.J. van den Bent, M. Weller, B. Fisher, M.J. Taphoorn, K. Belanger, A.A. Brandes, C. Marosi, U. Bogdahn, J. Curschmann, R.C. Janzer, S.K. Ludwin, T. Gorlia, A. Allgeier, D. Lacombe, J.G. Cairncross, E. Eisenhauer, R.O. Mirimanoff, European Organisation for Research and Treatment of Cancer Brain Tumor and Radiotherapy Groups, National Cancer Institute of Canada Clinical Trials Group, Radiotherapy plus concomitant and adjuvant temozolomide for glioblastoma, *New Engl. J. Med.* 352 (2005) 987–996.
- [7] D.R. Groothuis, The blood–brain and blood–tumor barriers: a review of strategies for increasing drug delivery, *Neurol. Oncol.* 2 (2000) 45–59.
- [8] R.A. Kroll, E.A. Neuwelt, Outwitting the blood–brain barrier for therapeutic purposes: osmotic opening and other means, *Neurosurgery* 42 (1998) 1083–1099.
- [9] K. Matsukado, T. Inamura, S. Nakano, M. Fukui, R.T. Bartus, K.L. Black, Enhanced tumor uptake of carboplatin and survival in glioma-bearing rats by intracarotid infusion of bradykinin analog, RMP-7, *Neurosurgery* 39 (1996) 125–133.
- [10] K.A. Walter, R.J. Tamargo, A. Olivi, P.C. Burger, H. Brem, Intratumoral chemotherapy, *Neurosurgery* 37 (1995) 1128–1145.
- [11] R.H. Bobo, D.W. Laske, A. Akbasak, P.F. Morrison, R.L. Dedrick, E.H. Oldfield, Convection-enhanced delivery of macromolecules in the brain, *Proc. Natl. Acad. Sci. USA* 91 (1994) 2076–2080.
- [12] J.N. Bruce, A. Falavigna, J.P. Johnson, J.S. Hall, B.D. Birch, J.T. Yoon, E.X. Wu, R.L. Fine, A.T. Parsa, Intracerebral clysis in a rat glioma model, *Neurosurgery* 46 (2000) 683–691.
- [13] M.G. Kaiser, A.T. Parsa, R.L. Fine, J.S. Hall, I. Chakrabarti, J.N. Bruce, Tissue distribution and antitumor activity of topotecan delivered by intracerebral clysis in a rat glioma model, *Neurosurgery* 47 (2000) 1391–1399.
- [14] J.W. Degen, S. Walbridge, A.O. Vortmeyer, E.H. Oldfield, R.R. Lonser, Safety and efficacy of convection-enhanced delivery of gemcitabine or carboplatin in a malignant glioma model in rats, *J. Neurosurg.* 99 (2003) 893–898.
- [15] Z. Lidar, Y. Mardor, T. Jonas, R. Pfeffer, M. Faibel, D. Nass, M. Hadani, Z. Ram, Convection-enhanced delivery of paclitaxel for the treatment of recurrent malignant glioma: a phase I/II clinical study, *J. Neurosurg.* 100 (2004) 472–479.
- [16] S. Sugiyama, Y. Yamashita, T. Kikuchi, R. Saito, T. Kumabe, T. Tominaga, Safety and efficacy of convection-enhanced delivery of ACNU, a hydrophilic nitrosourea, in intracranial brain tumor models, *J. Neurooncol.* 82 (2007) 41–47.
- [17] S. Sugiyama, Y. Yamashita, T. Kikuchi, Y. Sonoda, T. Kumabe, T. Tominaga, Enhanced antitumor effect of combined-modality treatment using convection-enhanced delivery of hydrophilic nitrosourea with irradiation or systemic administration of temozolomide in intracranial brain tumor xenografts, *Neurol. Res.* 30 (2008) 960–967.
- [18] R. Saito, Y. Sonoda, T. Kumabe, K. Nagamatsu, M. Watanabe, T. Tominaga, Regression of recurrent glioblastoma infiltrating the brain stem after convection-enhanced delivery of nimustine hydrochloride, *J. Neurosurg. Pediatr.* 7 (2011) 522–526.
- [19] K.S. Bankiewicz, J.L. Eberling, M. Kohutnicka, W. Jagust, P. Pivrotto, J. Bringas, J. Cunningham, T.F. Budinger, J. Harvey-White, Convection-enhanced delivery of AAV vector in parkinsonian monkeys; in vivo detection of gene expression and restoration of dopaminergic function using pro-drug approach, *Exp. Neurol.* 164 (2000) 2–14.
- [20] R. Saito, J.R. Bringas, T.R. McKnight, M.F. Wendland, C. Mamot, D.C. Drummond, D.B. Kirpotin, J.W. Park, M.S. Berger, K.S. Bankiewicz, Distribution of liposomes into brain and rat brain tumor models by convection-enhanced delivery monitored with magnetic resonance imaging, *Cancer Res.* 64 (2004) 2572–2579.
- [21] P.H. Chan, G.Y. Yang, S.F. Chen, E. Carlson, C.J. Epstein, Cold-induced brain edema and infarction are reduced in transgenic mice overexpressing CuZn-superoxide dismutase, *Ann. Neurol.* 29 (1991) 482–486.
- [22] K. Murakami, T. Kondo, S. Sato, Y. Li, P.H. Chan, Occurrence of apoptosis following cold injury-induced brain edema in mice, *Neuroscience* 81 (1997) 231–237.
- [23] R.D. Arnold, D.E. Mager, J.E. Slack, R.M. Straubinger, Effect of repetitive administration of doxorubicin-containing liposomes on plasma pharmacokinetics and drug biodistribution in a rat brain tumor model, *Clin. Cancer Res.* 11 (2005) 8856–8865.
- [24] U.S. Sharma, A. Sharma, R.I. Chau, R.M. Straubinger, Liposome-mediated therapy of intracranial brain tumors in a rat model, *Pharm. Res.* 14 (1997) 992–998.
- [25] C. Adamson, O.O. Kanu, A.I. Mehta, C. Di, N. Lin, A.K. Mattox, D.D. Bigner, Glioblastoma multiform: a review of where we have been and where we are going, *Expert Opin. Invest. Drugs* 18 (2009) 1061–1083.
- [26] R. Saito, T. Kumabe, M. Kanamori, Y. Sonoda, T. Tominaga, Dissemination limits the survival of patients with anaplastic ependymoma after extensive surgical resection, meticulous follow up, and intensive treatment for recurrence, *Neurosurg. Rev.* 33 (2010) 185–191.
- [27] M.M. Patel, B.R. Goyal, S.V. Bhadada, J.S. Bhatt, A.F. Amin, Getting into the brain: approaches to enhance brain drug delivery, *CNS Drugs* 23 (2009) 35–58.
- [28] N.A. Vick, J.D. Khandekar, D.D. Bigner, Chemotherapy of brain tumors, *Arch. Neurol.* 34 (1977) 523–526.
- [29] H. Nakagawa, D.R. Groothuis, E.S. Owens, J.D. Fenstermacher, C.S. Patlak, R.G. Blasberg, Dexamethasone effects on 125I-albumin distribution in experimental RG-2 gliomas and adjacent brain, *J. Cereb. Blood Flow Metab.* 7 (1987) 687–701.